J. Math. Anal. Appl. 400 (2013) 222–238

Contents lists available at SciVerse ScienceDirect

Journal of Mathematical Analysis and Applications

journal homepage: www.elsevier.com/locate/jmaa

Analysis of a causal diffusion model and its backwards diffusion problem

Richard Kowar

Department of Mathematics, University of Innsbruck, Technikerstrasse 21a/2, A-6020, Innsbruck, Austria

ARTICLE INFO

Article history:
Received 6 March 2012
Available online 30 November 2012
Submitted by Hyeonbae Kang

Keywords:
Causal diffusion
Backwards diffusion problem
Irreversibility
Particle method
Landweber method

ABSTRACT

In Kowar (2012) [25] a diffusion model was developed and analyzed that obeys causality, i.e. the speed of propagation of the concentration is finite. In this article we analyze the respective causal backwards diffusion problem. The motivation for this paper is that because real diffusion obeys causality, a causal diffusion model may contain smaller modeling errors than the noncausal standard model and thus an increase of resolution of inverse and ill-posed problems related to diffusion is possible. We derive an analytic representation of the Green function of causal diffusion in the $\mathbf{k} - t$-domain (wave vector-time domain) that enables us to analyze the properties of the causal backwards diffusion problem. In particular, it is proven that this inverse problem is ill-posed, but not exponentially ill-posed. Furthermore, a theoretical and numerical comparison between the standard diffusion model and the causal diffusion model is performed. The paper is concluded with numerical simulations of the backwards diffusion problem via the Landweber method that confirm our theoretical results.

1. Introduction

Inverse problems related to diffusion belong to a very important field of applications. Such and similar problems are studied in the articles [1–14] and books [15–24] to name but a few. Since these inverse problems are *ill-posed*, *data* and *qualitative modeling errors* have a strong impact on the numerical solution. Hence if the diffusion model, the direct problem, is qualitatively improved, then it is possible to increase the resolution of related inverse problems. Since real diffusion has a finite diffusion speed, it is possible that the causal diffusion model developed in [25] has smaller modeling errors than the noncausal standard diffusion model. (Of course this can be verified by experiment only.) In this paper we focus on the analysis of the backwards diffusion problem corresponding to the *causal* diffusion model (direct problem) presented in [25]. In order to describe the goal of this paper, we start with a short description of the direct problem.

1.1. The direct problem

Let v denote the concentration of a substance diffusing with constant speed c and *initial concentration* u. We show that the causal diffusion model developed in [25] has the following analytic representation[1]

$$\hat{v}(\mathbf{k}, m+s) = (2\pi)^{-N/2} \Upsilon_N(|\mathbf{k}|)^m \Upsilon_N(|\mathbf{k}|\, s) \hat{u}(\mathbf{k}) \tag{1}$$

E-mail address: richard.kowar@uibk.ac.at.

[1] We will see that causal diffusion is determined by the speed of diffusion c, a time period τ and the space dimension N. Here we assume $c = 1$ and $\tau = 1$.

0022-247X/$ – see front matter
doi:10.1016/j.jmaa.2012.11.041

for $\mathbf{k} \in \mathbb{R}^N$ ($N \in \mathbb{N}$), $m \in \mathbb{N}_0$ and $s \in (0, 1]$, where $\hat{v}$ denotes the Fourier transform of v with respect to $\mathbf{x} \in \mathbb{R}^N$ and Υ_N is the solution of

$$\Upsilon_N''(t) + \frac{(N-1)}{t}\,\Upsilon_N'(t) + \Upsilon_N(t) = 0 \quad t > 0, \tag{2}$$

with initial conditions

$$\Upsilon_N(0+) = 1 \quad \text{and} \quad \Upsilon_N'(0+) = 0. \tag{3}$$

For example, for $N = 1, 2, 3$ we have

$$\Upsilon_1(t) = \cos(t), \qquad \Upsilon_2(t) = \mathrm{J}_0(t) \quad \text{and} \quad \Upsilon_3(t) = \operatorname{sinc}(t), \tag{4}$$

where J_0 denotes the *Bessel function* of first kind and order zero (cf. [26]). Here $\check{\Upsilon}(\cdot, s)$ denotes the inverse Fourier transform of $\Upsilon(|\cdot|s)$.

1.2. The inverse problem

The respective backwards diffusion problem corresponds to the estimation of the *initial concentration* $u = u(\mathbf{x})$ for given concentration $w = w(\mathbf{x}) = v(\mathbf{x}, T)$ at time T. Mathematically this corresponds to the solution of the Fredholm integral equation of the first kind

$$F_T(u) = w \quad \text{for given data } w,$$

where the forward operator is defined by $F_T(u) := v(\cdot, T)$ with v as in (1) and $T > 0$ denotes the *data acquisition time*. We show (for appropriate spaces) that the forward operator is injective and that it is compact

(1) if $N = 2$ and $T > 2\,\tau$ and
(2) if $N \geq 3$ and $T > \tau$,

where N denotes the *space dimension* and t the time. In contrast to the standard diffusion model, the forward operator F_T is not compact for $N = 1$. Moreover, we show that the envelope of the Fourier transform of $F_T(u)$ does not decrease exponentially fast. In this sense the inverse problem is *not* exponentially ill-posed.

1.3. Irreversibility and time reversal

Numerical simulations for $N = 2$ indicate that the backwards diffusion problem is practically solvable for data acquisition time $T < \tau$ but not for $T \geq 3\tau$. This observation can be explained as follows: In [25, cf. Lemma 4 and Proposition 2] it is shown that v solves a hyperbolic equation of second order on each time interval $(n\tau, (n+1)\tau)$ for $n \in \mathbb{N}_0$ with "initial conditions"

$$v(\cdot, n\,\tau) = v(\cdot, n\,\tau+) \quad \text{and} \quad \frac{\partial v}{\partial t}(\cdot, n\,\tau+) = 0 \quad \left(\neq \frac{\partial v}{\partial t}(\cdot, n\,\tau-)\right).$$

But this means that – in contrast to the standard diffusion model (with exact data) – the technique of *time reversal* is not applicable, because the following initial data for the time reversal ($t \in [0, T] \to T - t$)

$$\frac{\partial v}{\partial t}(\cdot, \tau-),\ \frac{\partial v}{\partial t}(\cdot, 2\,\tau-),\ \ldots,\ \frac{\partial v}{\partial t}(\cdot, m\,\tau-),\ \ldots$$

cannot be acquired. If the data acquisition time satisfies $T < \tau$, then the (single) missing second initial data causes ill-posedness of the backwards diffusion problem, but if $T \approx m\tau$ with large $m \in \mathbb{N}$ than the backwards diffusion problem is unsolvable (even for zero noise). We consider this form of irreversibility of our diffusion model more physically reasonable than that one of the standard diffusion model.

In particular, this shows that a time reversal method cannot be used to solve the causal backwards diffusion problem studied in this paper. Therefore the numerical solution of the causal backwards diffusion problem is solved with an iterative regularization method.

The paper is organized as follows. In Section 2 we present our causal model of diffusion and derive those properties of diffusion that are needed for this paper. For the convenience of the reader we put the technical part in the Appendix. Comparisons between the standard diffusion model and our causal diffusion model are performed in Section 3. The theoretical and numerical aspects of the backwards diffusion problem are investigated in Sections 4 and 5. Numerical simulations of the inverse problem via the Landweber method are presented at the end of Section 5. The paper is concluded with a section of conclusion.

2. Causal diffusion and its properties

We start with the motivation of our model. It is well-known that standard diffusion belongs to the following class of problems: the concentration satisfies a scalar-valued evolution equation

$$\frac{\partial v}{\partial t} - \mathcal{A}\, v = 0 \quad t > 0 \text{ with } v|_{t=0} = u,$$

where $\mathcal{A}$ is a space convolution operator and the infinitesimal generator of a strongly continuous semigroup. In [25] it was proven, that the Green function G of such an evolution equation does not satisfy causality condition

$$\operatorname{supp}(G) \subseteq \{(\mathbf{x}, t) \in \mathbb{R}^N \times [0, \infty) \mid |\mathbf{x}| \le c\, t\} \tag{5}$$

for any $c > 0$, i.e. for an initial concentration $u(\mathbf{x}) = \delta(\mathbf{x})$ at time $t = 0$, the concentration is not zero outside the ball $\overline{B_{c\,t}(\mathbf{0})}$ after the time period t. As a consequence, we concluded that the semigroup property holds only for a discrete set of time instants $\{m\,\tau \mid m \in \mathbb{N}_0\}$, where τ is sufficiently small (cf. Theorem 1). If τ is sufficiently small, then the causal diffusion and the standard diffusion model will lead to similar results, in particular Fick's law is approximately satisfied for our diffusion model (compare Figs. 2 and 3 and cf. [25]). We emphasize that small modeling errors play no role for the direct problem, but they are important for the resolution of related inverse problems.

We now define *causal diffusion* for the case of a *constant* speed $c \in (0, \infty)$ and then summarize its basic properties.

Definition 1. Let $c, \tau \in (0, \infty)$, $\mathrm{d}\sigma(\mathbf{x}')$ denote the Lebesgue surface measure on $\mathbb{R}^N$ and $|S_R(\mathbf{0})|$ denote the surface area of the sphere $S_R(\mathbf{0})$. Diffusion with a constant speed c is defined by

$$v_{c,\tau}(\mathbf{x}, t) = \int_{S_{R(t)}(\mathbf{x})} \frac{v_{c,\tau}\left(\mathbf{x}', \tau_{n(t)}\right)}{|S_{R(t)}(\mathbf{0})|} \mathrm{d}\sigma(\mathbf{x}') \quad \text{with } v_{c,\tau}|_{t=0} = u, \tag{6}$$

where $\tau_{n(t)} := n(t)\tau$ and

$$n(t) \in \mathbb{N}_0 \quad \text{such that } t \in (n(t)\,\tau, (n(t)+1)\,\tau],$$

and $R(t) := c\,(t - n(t)\,\tau)$. If $u(\mathbf{x}) = \delta(\mathbf{x})$, then we call $G_{c,\tau} := v_{c,\tau}$ the Green function of diffusion. Here $\delta(\mathbf{x})$ denotes the *delta distribution* on $\mathbb{R}^N$.

In the following theorem, we summarize some results derived in [25, cf. Lemma 2, Theorem 4, Propositions 1, 4, 2 and Lemma 4].

Theorem 1. *For $c,\ \tau > 0$ let $G_{c,\tau}$ and $v_{c,\tau}(\mathbf{x}, t)$ be defined as in Definition 1 and $u \in L^1(\mathbb{R}^N)$.*

(a) *The* forward operator

$$F_T : L^1(\mathbb{R}^N) \to L^1(\mathbb{R}^N), \qquad u \mapsto v_{c,\tau}(\mathbf{x}, T) \quad (T > 0 \textit{ fixed}) \tag{7}$$

is well-defined and we have $\|u\|_{L^1} = \|v_{c,\tau}\|_{L^1}$. The last property means that conservation law of mass *holds.*

(b) *Let S_τ denote the space convolution operator*

$$S_\tau\, u := G(\cdot, \tau) *_{\mathbf{x}} u \quad \textit{for } u \in L^1(\mathbb{R}^n).$$

Then we have

$$v_{c,\tau}(\cdot, t) = S_\tau^m\, S_s\, u \quad \textit{for } t = \tau_m + s,\ s \in (0, \tau]. \tag{8}$$

(c) *The Green function satisfies causality condition (5).*

Remark 1. The reader may object that the above model of causal diffusion is not derived from first principles. The derivation of our model from microscopic equations is intended to be carried out in the future.

In order to analyze the backwards diffusion problem corresponding to our diffusion model, we need the Fourier representation of the Green function $G_{c,\tau}$. In this paper $\hat{f}(\mathbf{k})$ and $\mathcal{F}\{f\}(\mathbf{k})$ denote the Fourier transform of $\mathbf{x} \in \mathbb{R}^N \mapsto f(\mathbf{x})$. Our definition of the Fourier transform and the respective Convolution Theorem are formulated at the beginning of the Appendix.

Theorem 2. *Let $c,\ \tau > 0$, $G_{c,\tau}$ and Υ_N be defined as in Definition 1 and (18) (cf. Appendix), respectively. Then*

$$\hat{G}_{c,\tau}(\mathbf{k}, s) = \frac{\Upsilon_N(|\mathbf{k}|\, c\, s)}{(2\,\pi)^{N/2}} \quad \textit{for } \mathbf{k} \in \mathbb{R}^N,\ s \in (0, \tau] \tag{9}$$

and $\mu_s(A) := \int_A G_{c,\tau}(\mathbf{x}, s)\, \mathrm{d}\mathbf{x}$ defines a positive measure on the Borel sets. Moreover, (2), (4) and (20) (cf. Appendix) hold, and the semigroup properties (8) is equivalent to

$$\hat{v}_{c,\tau}(\cdot, t) = (2\,\pi)^{-N/2}\, \Upsilon_N(|\cdot|\, c\, \tau)^m\, \Upsilon_N(|\cdot|\, c\, s)\hat{u}. \tag{10}$$

Proof. We note that $s \in (0, \tau]$ implies $n(s) = 0$ and $R(s) = c\,\tau$. Moreover, we have

$$\int_{S_R(\mathbf{x})} f(\mathbf{x}')\,\mathrm{d}\,\sigma(\mathbf{x}') \equiv \int_{S_1(\mathbf{0})} f(\mathbf{x} + R\,\mathbf{y})\,R^{N-1}\,\mathrm{d}\,\sigma(\mathbf{y}),$$
$$|S_R(\mathbf{0})| = |S_1(\mathbf{0})|\,R^{N-1}.$$

From these facts and Definition 1 with $u(\mathbf{x}) = \delta(\mathbf{x})$, it follows that

$$G_{c,\tau}(\mathbf{x}, s) = \int_{S_{R(s)}(\mathbf{x})} \frac{\delta(\mathbf{x}')}{|S_{R(s)}(\mathbf{0})|}\,\mathrm{d}\sigma(\mathbf{x}') = \int_{S_1(\mathbf{0})} \frac{\delta(\mathbf{x} + R(s)\,\mathbf{y})}{|S_1(\mathbf{0})|}\,\mathrm{d}\sigma(\mathbf{y}).$$

$\mu_s(A)$ is a positive measure, since $G_{c,\tau}(\mathbf{x}, s)$ is a positive distribution.

To determine the Fourier transform of $G_{c,\tau}$, we use the following series representation derived in Lemma 2 (cf. Appendix):

$$(2\,\pi)^{N/2}\,\mathcal{F}\left\{\int_{S_1(\mathbf{0})} \frac{\delta(\cdot + c\,s\,\mathbf{y})}{|S_1(\mathbf{0})|}\,\mathrm{d}\sigma(\mathbf{y})\right\}(\mathbf{k}) = \sum_{j=0}^{\infty}(-1)^j \cdot a_{2j} \cdot (|\mathbf{k}|\,c\,s)^{2j}$$

for $s \in (0, \tau]$ with $a_0 = 1$ and

$$a_{2j} = \frac{1}{(2j)!}\,\frac{1 \cdot 3 \cdot 5 \cdots (2j-1)}{N \cdot (N+2) \cdot (N+4) \cdots (N+2j-2)} \quad \text{for } j \in \mathbb{N}.$$

In Theorem 9 it is shown that $\Upsilon_1(t) = \cos(t)$, $\Upsilon_2(t) = \mathrm{J}_0(|\mathbf{k}|\,c\,s)$ and (20) holds. $\Upsilon_3(t) = \mathrm{sinc}(t)$ can be concluded from Theorem 9, too, or alternatively from

$$a_{2j} = \frac{1}{(2j)!}\,\frac{1 \cdot 3 \cdot 5 \cdots (2j-1)}{3 \cdot 5 \cdot 7 \cdots (2j+1)} = \frac{1}{(2j+1)!}.$$

The equivalence of the representation (10) and the semigroup properties (8) follows from Theorem 2 and the Convolution Theorem.

Finally, the differential equation (2) follows from the series representation of Υ. This concludes the proof. □

3. Comparison of standard diffusion and causal diffusion

In this section, the standard diffusion model and our causal diffusion model are compared in the space–time domain. We show that for an appropriate parameter set a discretization of the standard diffusion equation can yield a similar result as the causal diffusion model introduced in Definition 1.

In the following we denote the Green function of standard diffusion by $G_{\infty,0}$, since we can associate c and τ the values $c = \infty$ and $\tau = 0$ (cf. Remark 2). Similarly we use the notation

$$v_{\infty,0} := G_{\infty,0} *_{\mathbf{x}} u \quad \text{for } u \in L^1(\mathbb{R}^N).$$

In order to keep the formulas and equations short, we focus on the two dimensional case. Consider the diffusion of an image with size of pixel $(\Delta x)^2$ and size of time step $\Delta t := \tau$. We use the notion

$$v_{i,j}^m := v(i\,\Delta x, j\,\Delta x, \tau_m) \quad \text{for } i, j \in \mathbb{Z} \text{ and } m \in \mathbb{N}_0.$$

If the length of an image pixel Δx satisfies (cf. Definition 1)

$$R(\tau) = c\,\tau \equiv \Delta x,$$

then we can use the rough approximation

$$\int_{|\mathbf{x}-\mathbf{y}|=R(\tau)} \frac{f(\mathbf{x}')}{|S_1(\mathbf{0})|}\,\mathrm{d}\sigma(\mathbf{y}) \approx (f_{i+1,j} + f_{i-1,j} + f_{i,j+1} + f_{i,j-1})/4.$$

With this *rough* discretization the causal diffusion model (6) is equivalent to

$$v_{i,j}^{n+1} = \frac{1}{4}\left[v_{i+1,j}^n + v_{i-1,j}^n + v_{i,j+1}^n + v_{i,j-1}^n\right],$$

which can be reformulated as follows

$$\frac{v_{i,j}^{n+1} - v_{i,j}^n}{\tau} = \frac{\Delta x^2}{4\,\tau}\left[\frac{v_{i+1,j}^n - 2\,v_{i,j}^n + v_{i-1,j}^n}{\Delta x^2} + \frac{v_{i,j+1}^n - 2\,v_{i,j}^n + v_{i,j-1}^n}{\Delta x^2}\right]. \tag{11}$$

But this is the *Forward Euler method of the classical diffusion equation.*

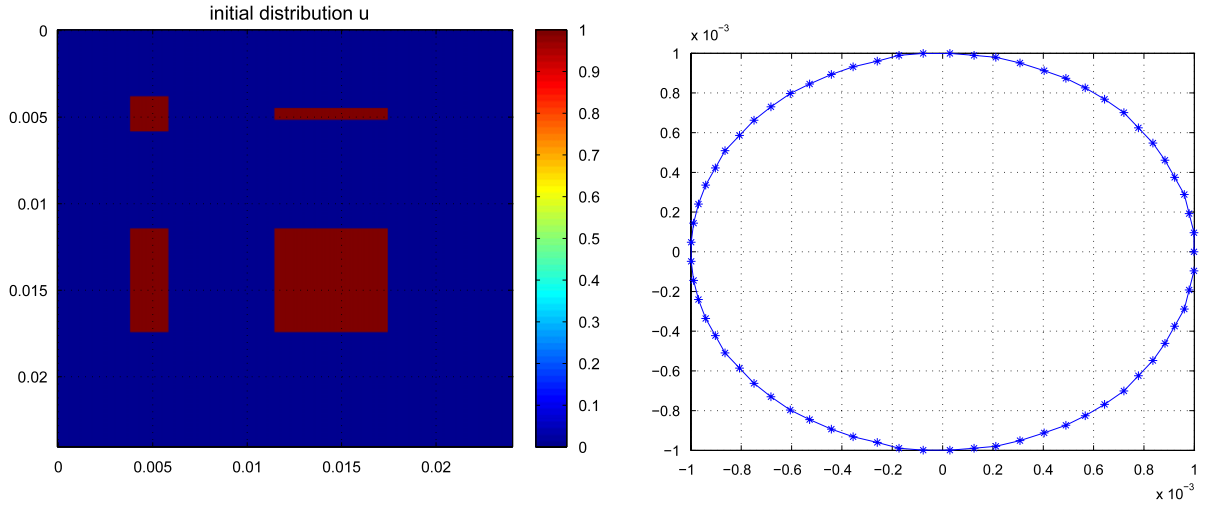

Fig. 1. The left picture shows the initial distribution u and the right picture visualizes the discretization of the circle of radius $R = R(\tau)$ that is used to evaluate the circle integrals in Definition 1.

Remark 2. From this finite difference equation, the classical diffusion equation can be obtained for $\tau \to 0$ under the side condition $\Delta x^2/(4\tau) = \text{const}$, i.e. the diffusivity corresponds to

$$D_0 = \frac{c^2\,\tau}{2N} \quad \text{with } c := \frac{\Delta x}{\tau} \text{ and } N = 2. \tag{12}$$

Carrying out this limit process yields $c = \infty$, i.e. the diffusion speed can be interpreted as infinite.

The following numerical example indicates that for *sufficiently large time t* the forward Euler method (with fine space discretization) can be considered as a noncausal approximation of the causal diffusion model.

Example 1. We choose the following values

$$c = 6.3 \cdot 10^{-3}\ \text{m/s}, \qquad R := R(\tau) := 10^{-3}\ \text{m} \quad \text{and} \quad \tau := R/c.$$

From (12) it follows that

$$D_0 \equiv c^2\,\tau/4 = 1.575 \cdot 10^{-6}\ \text{m}^2/\text{s}.$$

The initial mass distribution is shown in Fig. 1. $v_{c,\tau}$ is calculated via Definition 1 with circles discretized by 65 points (cf. Fig. 1). The noncausal distribution $v_{\infty,0}$ was calculated via the forward Euler method for the standard diffusion equation with discretization

$$\Delta x := R/10 \quad \text{and} \quad \Delta t := \frac{\Delta x^2}{2N\,D_0}$$

such that

$$\frac{\Delta x^2}{2N\,\Delta t} \geq D_0 \quad \text{(convergence condition)}$$

holds. A time sequence of $v_{c,\tau}(\cdot,t)$ and $v_{\infty,0}(\cdot,t)$ for the time instants $t = \frac{\tau}{3}, \frac{2\tau}{3}, \tau, \ldots, 2\tau$ is visualized in Figs. 2 and 3, respectively. As expected each distribution $v_{\infty,0}(\cdot,t)$ is very smooth, in contrast to the distribution $v_{c,\tau}(\cdot,t)$ of causal diffusion. No edge or corner appears in the case of standard diffusion. Although it is not visible, in contrast to $v_{c,\tau}(\cdot,t)$, the support of $v_{\infty,0}(\cdot,t)$ does not lie within the image.

4. Basic properties of the forward operator

The calculation of a diffusing substance over the time period T with initial concentration $u \in L^1(\mathbb{R}^N)$ corresponds to the evaluation of the forward operator (7). We define this as the direct problem and consider the estimation of the initial concentration u from appropriate data w. That is to say the solution of the Fredholm integral equation of the first kind

$$F_T(u) = w \quad \text{for given data } w. \tag{13}$$

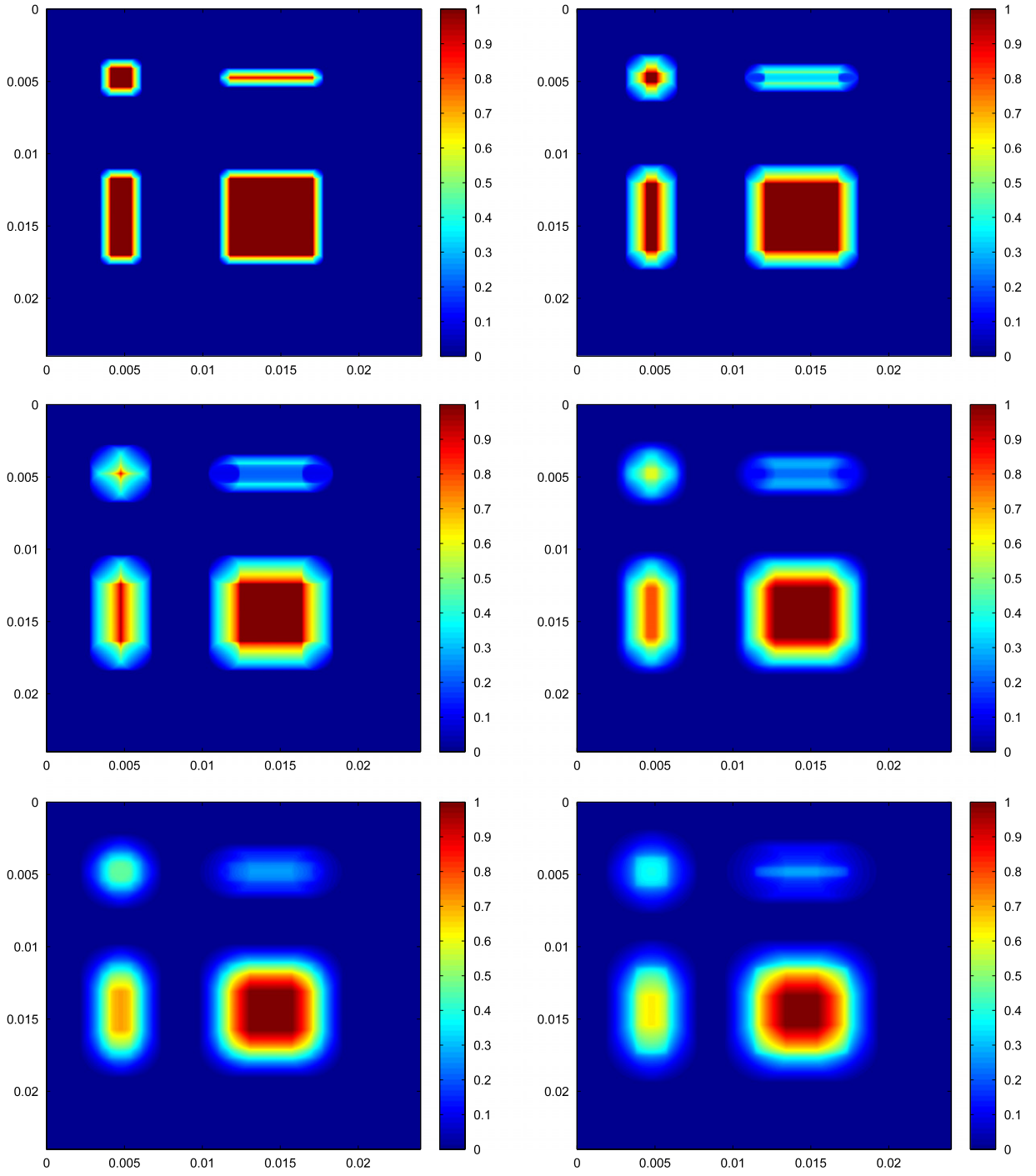

Fig. 2. Visualization of causal diffusion for the time sequence $(\frac{\tau}{3}, \frac{2\tau}{3}, \tau, \ldots, 2\tau)$ with discretization $\Delta x = 9.6 \cdot 10^{-6}$ and $\Delta t = \tau = R/c$. The initial distribution is shown in Fig. 1.

This inverse problem requires the knowledge of c, τ and T. In this section we investigate the properties of the forward operator and in the subsequent section we discuss and perform numerical simulations of the inverse problem. We use the notation:

Definition 2. (a) Let $T > 0$ and $r > 0$. Then we define $\Omega_T := B_{r+cT}(\mathbf{0})$ for $T > 0$, where $B_r(\mathbf{0})$ denotes the open ball with center $\mathbf{0}$ and radius r.
(b) $L^2_c(\mathbb{R}^N)$ is defined as the space of L^2-functions with compact support in $\mathbb{R}^N$.

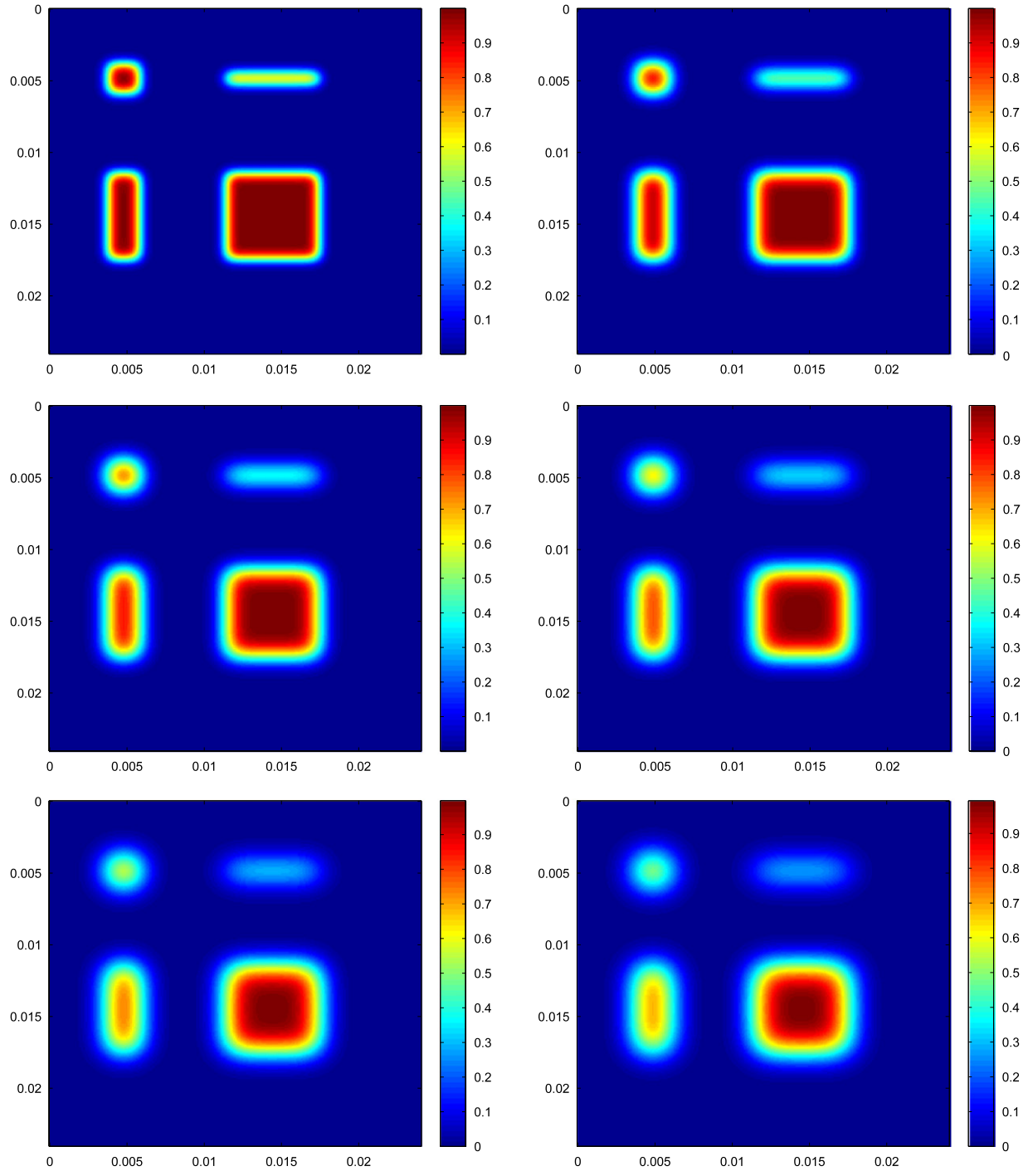

Fig. 3. Visualization of standard diffusion for the time sequence $(\frac{\tau}{3}, \frac{2\tau}{3}, \tau, \ldots, 2\tau)$ with discretization $\Delta x := R/10$ and $\Delta t := \frac{\Delta x^2}{2ND_0}$. The initial distribution is shown in Fig. 1.

Theorem 3. *Let $T > 0$ and $G_{c,\tau}$ be as in Definition 1. The sets of zeros of $\hat{G}_{c,\tau}(\cdot, T)$ is discrete and countably infinite, and the operator $F_T : L^1_c(\mathbb{R}^N) \to L^1_c(\mathbb{R}^N)$ is injective.*

Proof. (a) For $t = \tau_n + s$ with $n \in \mathbb{N}_0$ and $s \in (0, \tau]$, we have $\hat{G}_{c,\tau}(\mathbf{k}, \tau_n + s) = \hat{G}_{c,\tau}(\mathbf{k}, \tau)^n \hat{G}_{c,\tau}(\cdot, s)$. Hence it is sufficient to show that the sets of zeros of $\hat{G}_{c,\tau}(\cdot, s)$ is discrete and countably infinite. But this from Theorem 9 and the fact that $\Upsilon_1(s) = \cos(s)$ and $\Upsilon_2(s) = \mathrm{J}_0(s)$ have discrete and countably infinite zeros.

(b) For the injectivity of F_T. Since u and $G_{c,\tau}(\cdot, T)$ have compact support, $\hat{u}$ and $\hat{G}_{c,\tau}(\cdot, T)$ exist and the Convolution Theorem holds (cf. Theorem 7.1.15 in [27]). Hence

$$\mathcal{F}\{F_T(u)\} = \hat{G}_{c,\tau}(\mathbf{k}, T)\,\hat{u}$$

which implies that

$$F_T(u) = 0 \Rightarrow u = 0$$

is equivalent to

$$\hat{G}_{c,\tau}(\cdot, T)\,\hat{u} = 0 \Rightarrow \hat{u} = 0.$$

From $\hat{G}_{c,\tau}(\cdot, T)\,\hat{u} = 0$ and part (a) of the proof we infer that $\hat{u}$ vanishes on a non-empty open set M. Because u has compact support, the Paley–Wiener Theorem implies that $\hat{u}$ can be extended to an analytic function $\hat{u}_{\text{ext}}$ on $\mathbb{C}^N$ satisfying $\hat{u}_{\text{ext}}(\mathbf{k}) = 0$ for $\mathbf{k} \in M$. Therefore $\hat{u}_{\text{ext}}$ is the zero function and consequently u vanishes. This proves that F_T is injective. □

Theorem 4. *The operator $F_T : L^2_c(\mathbb{R}^N) \to L^2_c(\mathbb{R}^N)$ is positive, linear and self-adjoint.*

Proof. First we show that $F_T : L^2_c(\mathbb{R}^N) \to L^2_c(\mathbb{R}^N)$ is well-defined. Because $L^2_c(\mathbb{R}^N)$ is a subspace of a Hilbert space, it is a Hilbert space, too. If $u \in L^2_c(\mathbb{R}^N)$, then $u \in L^1_c(\mathbb{R}^N)$ and thus $F_T(u) \in L^1(\mathbb{R}^N)$ by part (a) of Theorem 1. Since $G_{c,\tau}$ and u have compact support, their convolution exists and has compact support (cf. Theorem 7.1.15 in [27]). Hence we obtain $F_T(L^2_c(\mathbb{R}^N)) \subseteq L^1_c(\mathbb{R}^N)$. According to Parseval's formula and

$$|(2\pi)^{N/2}\,\hat{G}(\mathbf{k}, t)| \le C \quad \text{for some constant } C,$$

which follows from Theorem 9 (cf. Appendix) and Theorem 2, we have

$$\begin{aligned}\|F_T(u)\|^2_{L^2} &= (2\pi)^N \|\mathcal{F}\{F_T(u)\}\|^2_{L^2} = (2\pi)^N C \int_{\mathbb{R}^N} |\hat{G}(\mathbf{k}, t)\,\hat{u}(\mathbf{k})|^2 \,\mathrm{d}\mathbf{k} \\ &\le C\,\|u\|^2_{L^2} < \infty,\end{aligned}$$

i.e. $F_T(u) \in L^2_c(\mathbb{R}^N)$. Hence the operator is well-defined.

The positivity and linearity of the operator F_T follows at once from Definition 1 and Theorem 1, respectively.

Since $G_{c,\tau}(\mathbf{x} - \mathbf{x}', T) = G_{c,\tau}(\mathbf{x}' - \mathbf{x}, T)$, it follows that

$$\langle F_T(u), w\rangle_{L^2} = \int_{\mathbb{R}^N}\int_{\mathbb{R}^N} G_{c,\tau}(\mathbf{x} - \mathbf{x}', T) u(\mathbf{x}')\, w(\mathbf{x})\,\mathrm{d}\,\mathbf{x}'\,\mathrm{d}\,\mathbf{x} = \langle u, F_T(w)\rangle_{L^2}$$

for $w \in L^2_c(\mathbb{R}^N)$ and thus F_T is self-adjoint. This concludes the proof. □

Theorem 5. *If $N = 1$ and $T > 0$, then $G_{c,\tau}(\cdot, T)$ is a discrete and positive measure and the operator $F_T : L^2(\Omega_0) \to L^2(\Omega_T)$ is not compact.*

Proof. Without loss of generality we set $c = 1$. According to Theorem 2 we have for $s \in (0, \tau]$:

$$G_{c,\tau}(x, s) = \mathcal{F}^{-1}\{\cos(k\,s)\}(x) = \frac{1}{2}\,[\delta(x - s) + \delta(x + s)],$$

which implies that $G_{c,\tau}(x, T)$ is a convolution of positive distributions with singular support. Therefore $G_{c,\tau}(\cdot, T)$ corresponds to a discrete and positive measure. That F_T is not compact follows from the fact that

$$F_T = (R_\tau + L_\tau)^m\,(R_s + L_s) \quad \text{for } T = \tau_m + s,$$

where $R_s,\ L_s : L^2(\mathbb{R}) \to L^2(\mathbb{R})$ are noncompact operators defined by

$$R_s(u) := u(\cdot - s) \quad \text{and} \quad L_s(u) := u(\cdot + s). \quad \square$$

Theorem 6. *If $N = 2$ and $T > 2\,\tau$, then $G_{c,\tau}(\cdot, T) \in L^2_c(\mathbb{R}^2)$ and the operator $F_T : L^2(\Omega_0) \to L^2(\Omega_T)$ is compact.*

Proof. Without loss of generality we set $c = 1$. Let $T = \tau_m + s$ with $m \ge 2$ and $s \in (0, \tau]$. From Theorem 2 together with $|\mathrm{J}_0(r)| \le 1$ and the asymptotic behavior (23) of J_0 (cf. Appendix), we get for $N = 2$:

$$\begin{aligned}\|\hat{G}_{c,\tau}(\cdot, T)\|^2_{L^2(\mathbb{R}^2)} &= 2\pi \int_0^\infty \mathrm{J}_0^{2m}(r\,\tau)\,\mathrm{J}_0^2(r\,s)\,r\,\mathrm{d}\,r \\ &\le A + \frac{2^3}{\pi\,\tau\,s}\int_M^\infty \frac{1}{r^2}\,\mathrm{d}\,r,\end{aligned}$$

where

$$A := 2\,\pi \int_0^M \mathrm{J}_0^{2\,m}(r\,\tau)\,\mathrm{J}_0^2(r\,s)\,r\,\mathrm{d}\,r < \infty$$

and $M > 0$. Because of $\int_M^\infty 1/r^2\,\mathrm{d}\,r = 1/M$, we arrive at

$$\|\hat{G}_{c,\tau}(\cdot,T)\|^2_{L^2(\mathbb{R}^2)} = A + \frac{2^3}{\pi\,\tau\,s}\,\frac{1}{M} < \infty,$$

i.e. $\hat{G}_{c,\tau}(\cdot,T)$ lies in $L^2(\mathbb{R}^2)$. Consequently, $G_{c,\tau}(\cdot,T)$ lies in $L^2_c(\mathbb{R}^2)$. The compactness of the operator F_T (for $N = 2$ and $T > 2\,\tau$) follows from Theorem 8.15 in [28]. □

Theorem 7. *If $N \geq 3$ and $T > \tau$, then $G_{c,\tau}(\cdot,T) \in L^2_c(\mathbb{R}^3)$ and the operator $F_T : L^2(\Omega_0) \to L^2(\Omega_T)$ is compact.*

Proof. Without loss of generality we set $c = 1$. Let $T = \tau_m + s$ with $m \in \mathbb{N}$ and $s \in (0,\tau]$. From Theorem 2 and the estimation (21) in Theorem 9, it follows for $N \geq 3$:

$$\begin{aligned}\|\hat{G}_{c,\tau}(\cdot,T)\|^2_{L^2(\mathbb{R}^2)} &= |S_1(\mathbf{0})| \int_0^\infty \Upsilon_N^{2\,m}(r\,s)\,\Upsilon_N^2(r\,s)\,r^{N-1}\,\mathrm{d}\,r \\ &\leq |S_1(\mathbf{0})| \left(A + C_N^{2\,(m+1)} \int_M^\infty \frac{r^{N-1}}{(r\,s)^{(m+1)\,(N-1)}}\mathrm{d}\,r\right),\end{aligned}$$

where

$$A := |S_1(\mathbf{0})| \int_0^M \Upsilon_N^{2\,m}(r\,s)\,\Upsilon_N^2(r\,s)\,r^{N-1}\mathrm{d}\,r < \infty$$

and $M > 0$ is sufficiently large. Because of $\int_M^\infty r^{-(N-1)}\,\mathrm{d}\,r = -\frac{1}{(N-2)}\,M^{-(N-2)}$, we end up with

$$\|\hat{G}_{c,\tau}(\cdot,T)\|^2_{L^2(\mathbb{R}^2)} = |S_1(\mathbf{0})| \left(A + \frac{C_N^{2\,(m+1)}}{s^{(m+1)\,(N-1)}\,(N-2)\,M^{N-2}}\right) < \infty,$$

i.e. $\hat{G}_{c,\tau}(\cdot,T)$ lies in $L^2(\mathbb{R}^2)$. As a consequence, $G_{c,\tau}(\cdot,T)$ lies in $L^2_c(\mathbb{R}^2)$. The compactness of the operator F_T (for $N = 2$ and $T > 2\,\tau$) follows from Theorem 8.15 in [28]. □

From the Paley–Wiener–Schwartz Theorem (cf. [27]), it follows that the Moore–Penrose inverse $F^\dagger$ is uniquely defined by

$$F_T^\dagger := (F_\tau^\dagger)^m\,F_s^\dagger \quad (T = \tau_m + s, s \in (0,\tau])$$

with

$$\mathcal{F}\{F_s^\dagger(w)\}(\mathbf{k}) := \frac{\hat{w}(\mathbf{k})}{\hat{G}(\mathbf{k},s)}\,\chi_{\Omega_0(s)}(\mathbf{k}) \quad \text{for } \mathbf{k} \in \Omega_0(s). \tag{14}$$

Therefore if the data lies in

$$\mathcal{R}(F_T) := \left\{ w \in L^2_c(\mathbb{R}^N) \;\middle|\; \frac{\hat{w}}{\hat{G}(\cdot,\tau)^m\,\hat{G}(\cdot,s)} \in L^2(\mathbb{R}^N) \right\},$$

then the initial concentration u can be estimated in principle. In contrast to standard diffusion $\hat{G}(\mathbf{k},s)$ has countably infinite and discrete zeros (cf. Theorem 3). Hence it follows:

Corollary 1. *A necessary condition for $w \in \mathcal{R}(F_T)$ is that $\hat{w}$ has a zero of order $\geq m$ at k_* if $\hat{G}_{c,\tau}(\cdot,T)$ has a zero of order m at k_*.*

According to Theorem 9 for $N \in \mathbb{N}$ we have

$$\Upsilon_N(t) \asymp t^{(N-1)/2} \quad \text{for } t \to \infty$$

and thus the envelope of $\mathbf{k} \mapsto \hat{G}_{c,\tau}(\mathbf{k},T)$ decreases as

$$\mathbf{k} \mapsto a_T\,|\mathbf{k}|^{(\lfloor T/\tau\rfloor+1)\,(N-1)/2} \quad \text{for } |\mathbf{k}| \to \infty,$$

where

$$a_T := (c\,\tau)^{\lfloor T/\tau\rfloor\,(N-1)/2}\,(c\,(T - \lfloor T/\tau\rfloor\,\tau))^{(N-1)/2}.$$

Here $\lfloor a\rfloor$ denotes the largest integer $\leq a$ (and $m \equiv \lfloor T/\tau\rfloor$, $s \equiv T - \tau\,\lfloor T/\tau\rfloor$). Hence we get the following.

Corollary 2. *If $N = 2$ and $T > 2\tau$ or $N \geq 3$ and $T > \tau$, then the inverse problem (13) is ill-posed, but* not *exponentially ill-posed.*

5. Simulation of the inverse problem

5.1. Simulation of data via a particle method

In order to avoid an *inverse crime* we calculate the synthetic data for the inverse problem by a *particle method* (cf. [29]). One of the advantages of a particle method (as long as no mass flows over the boundary) is that the total mass is conserved. For simplicity we focus on the 2*D*-case and drop the subscripts c and τ in $G_{c,\tau}$ and $v_{c,\tau}$.

5.1.1. The particle method

The initial distribution u is approximated by an *image*, i.e. a piecewise constant function with quadratic pixels of length Δx. At time instant $t = \tau_{n-1}$ ($n \in \mathbb{N}$) the mass concentrated in a pixel separates in M parts and each part propagates on a straight line with constant speed c in a randomly chosen direction $\mathbf{d}$ during the time period τ. Here the directions are chosen with equal probability out of the set

$$\{A(\varphi)\,\mathbf{e}_1 \mid \varphi = 0,\ \pi/M, \ldots, (M-1)\,\pi/M\},$$

where $\mathbf{e}_1 := (1, 0)^T$ and $A(\varphi)$ denotes the matrix that rotates the argument about the angle φ in positive direction. This kind of data simulation allows that more than one "particle" go in the same direction such that a special type of noise is included in the simulated data. To each image pixel is then associated the number of all particles that lie within the pixel multiplied by $1/M$.

5.1.2. Noise

In order to avoid an inverse crime we perturbed the length of the radius $R(\tau) = c\,\tau$ by $\pm 0.25\%$ of its original length (uniformly distributed perturbation). In addition, uniformly distributed L^2-noise with positive mean value were added to the simulated data. As noise level we have chosen $\delta = 0.005$ (0.5%).

5.1.3. Convergence of the particle method

In the following we denote by $G[M](\mathbf{x}, t)$ the distribution simulated with the particle method and with initial distribution

$$\delta[M](\mathbf{x}) := \begin{cases} 1 & \text{if } \max(|x|, |y|) < \dfrac{\Delta x}{2} \\ 0 & \text{elsewhere.} \end{cases}$$

From analysis it is known that

$$\delta[M](\mathbf{x}) \overset{M\to\infty}{\longrightarrow} \delta(\mathbf{x}) \quad \text{and} \quad G[M](\mathbf{x}, t) \overset{M\to\infty}{\longrightarrow} G(\mathbf{x}, t) \quad \text{in } \mathcal{D}'(\mathbb{R}^2). \tag{15}$$

Here G denotes the Green function of causal diffusion (cf. Definition 1) and $\mathcal{D}'(\mathbb{R}^2)$ denotes the space of distributions on $\mathbb{R}^2$. We now show that the algorithm described above for an initial distribution u provides us with an approximate solution of $F_T(u)$, where F_T denotes the forward operator (7).

Theorem 8. *Let $u \in L^1_c(\mathbb{R}^2)$ and $v(\cdot, t) := G(\cdot, t) *_{\mathbf{x}} u$. For*

$$v[M](\cdot, t) := G[M](\cdot, t) *_{\mathbf{x}} u \quad (t > 0),$$

it follows that

$$v[M](\cdot, t) \overset{M\to\infty}{\longrightarrow} v(\cdot, t) \quad \text{in } L^1(\mathbb{R}^2).$$

Proof. Since the space $C_0^\infty(\mathbb{R}^2)$ is dense in $L^1(\mathbb{R}^2)$, we assume without loss of generality that $u \in C_0^\infty(\mathbb{R}^2)$. We have

$$\|v[M](\cdot, t) - v(\cdot, t)\|_{L^1} = \int_{\mathbb{R}^2} |f[M](\mathbf{x})|\,\mathrm{d}\mathbf{x}$$

with

$$f[M](\mathbf{x}) = \int_{\mathbb{R}^2} [G[M](\mathbf{x}', t) - G(\mathbf{x}', t)]u(\mathbf{x} - \mathbf{x}')\,\mathrm{d}\mathbf{x}'. \tag{16}$$

The function $f[M]$ is an element of $C_0^\infty(\mathbb{R}^2)$, since $G[M](\cdot, t) - G(\cdot, t)$ has compact support and $u \in C_0^\infty(\mathbb{R}^2)$ (cf. Proposition 32.1.1 in [30]). From (15) together with $u \in C_0^\infty(\mathbb{R}^2)$, it follows that the right hand side of (16) converges

pointwise and uniformly to zero on compact sets. This together with the fact that $f[M]$ has compact support implies

$$\|v[M](\cdot,t) - v(\cdot,t)\|_{L^1} \overset{M\to\infty}{\longrightarrow} 0.$$

As was to be shown. □

5.2. Numerical solution of the backwards diffusion problem

For solving the inverse problem we use the *Landweber method* (cf. e.g. [16–18,21]). Since $F_T : L^2_c(\mathbb{R}^N) \to L^2_c(\mathbb{R}^N)$ is a positive, linear and self-adjoint operator (cf. Theorem 4) the Landweber method reads as follows[2]

$$u_{n+1} = P\{u_n - \omega F_T[F_T(u_n) - w^\delta]\},$$

where ω denotes the *relaxation parameter*, w^δ denotes the noisy data and P denotes the orthogonal projection onto

$$\mathcal{R}(P) = \{u \in L^2 \mid u \geq 0\}.$$

The use of the projection operator guarantees that the solution is a positive (mass) distribution. As parameter choice rule we use the *discrepancy principle*, i.e. the iteration is stopped as soon as

$$\|F_T(u_{n+1}) - w^\delta\|_{L^2} < \eta\,\delta \quad (\eta \geq 2)$$

is true. The relaxation parameter was chosen as

$$\omega := \frac{1}{4}\,\frac{\|F_T(u_n) - w^\delta\|^2_{L^2}}{\|F_T[F_T(u_n) - w^\delta]\|^2_{L^2}}.$$

In order to avoid an inverse crime, the data w^δ is calculated by the particle method ($M = 65$) described above and the calculation of the Forward operator F_T in each iteration step is performed by integrals over circles (cf. Definition 1). Each circle is discretized by 50 points.

We now present two simulations of the backwards diffusion problem for $T = \tau$ and $T = 3\tau$, respectively.

Example 2. Consider the initial distribution shown in Fig. 4. This image consists of 682^2 quadratic pixels of length $\Delta x := 1/681$. As characteristic parameters of causal diffusion we have chosen $c = 1$ and $\tau = 8\,\Delta x/c$. Hence the characteristic radius $R(\tau)$ is 8 times Δx. As described above, the length of the radius $R(\tau)$ was randomly perturbed by $\pm 0.25\%$ of its original length. The data acquisition is performed at time $T = \tau$ and 0.5% (uniformly distributed) L^2-noise was added to the simulated data. The numerical results are visualized in Figs. 4 and 5. As expected, the estimation of large structures is much better than for smaller ones. Since the data acquisition is performed at a quite early time the estimation works well (for $t < \tau$ the forward operator is not compact). The discrepancy principle stops optimally for $\eta = 9.4$ after 6 steps.

Example 3. We consider the inverse problem from Example 2 again, but for the later data acquisition time $T = 3\tau$. The discrepancy principle stops optimally for $\eta = 5.9$ after 6 steps. As Fig. 6 shows it is not possible to restore the edges of the question mark, since the data are too much "smooth". This result reflects the ill-posedness of the problem (for $t > 2\tau$ the forward operator is compact).

6. Conclusions

The theoretical and numerical results of this paper show that the causal backwards diffusion problem is practically solvable for data acquisition time $T \leq \tau$ but not for $T \geq 3\tau$, where τ is a time period that characterizes causal diffusion (cf. Definition 1). Although the causal backwards diffusion problem is not exponentially ill-posed, the numerical solution of this problem is strongly limited by irreversibility. Indeed, as explained in Section 1.3, in order to perform a time reversal method, the set of data

$$\left\{\frac{\partial v}{\partial t}(\cdot, n\tau-) \mid n \in \mathbb{N}_0 \text{ and } n\tau < T\right\} \cup \left\{\frac{\partial v}{\partial t}(\cdot, T-)\right\}$$

is required which cannot be obtained by experiment.

Why are these facts not always numerically noticeable? This can be explained as follows. According to Section 3 the causal diffusion model with parameters c, τ and the discretized standard diffusion model with parameter D lead to similar results for time instants $t \geq \tau$ if

$$D = \frac{c^2\,\tau}{2N} \quad (N \text{ space dimension}).$$

[2] For simplicity, we write u_n, w^δ instead of $u_n[M]$, $w^\delta[M]$.

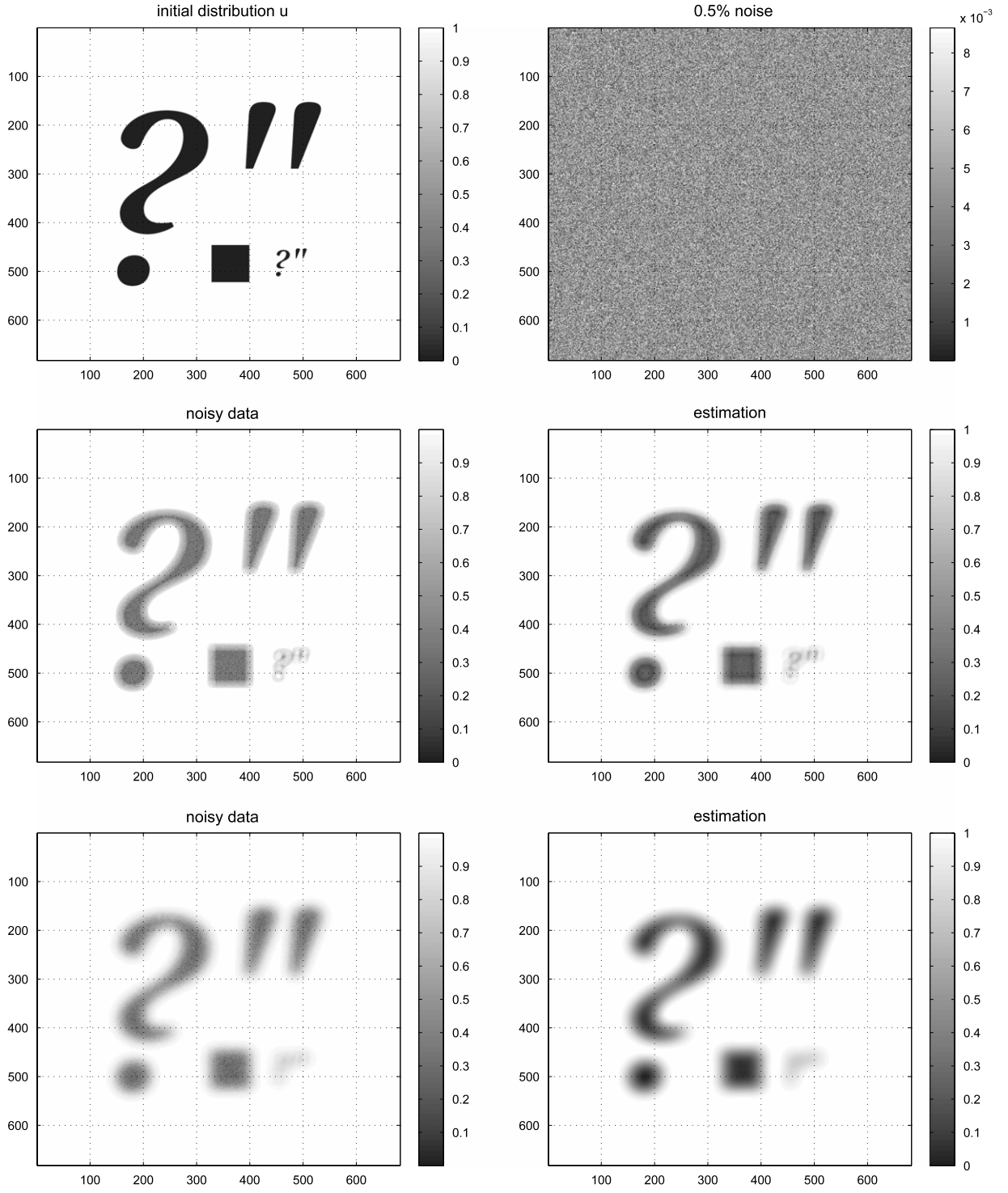

Fig. 4. Numerical solution of the inverse problem with 0.5% uniformly distributed L^2-noise for data acquisition time $T = \tau$ and $T = 3\tau$. For $T = \tau$ and $T = 3\tau$, the discrepancy principle stops optimally for $\eta = 9.4$ (6 steps) and $\eta = 5.9$ (6 steps), respectively.

Consider the discretized causal backwards diffusion problem for the two cases:

(1) $\Delta t \approx \tau \ll T$: the problem is "irreversible" and severe numerical problems are expected.
(2) $\Delta t \ll \tau = T$: the problem is "reversible" and no severe numerical problems are expected.

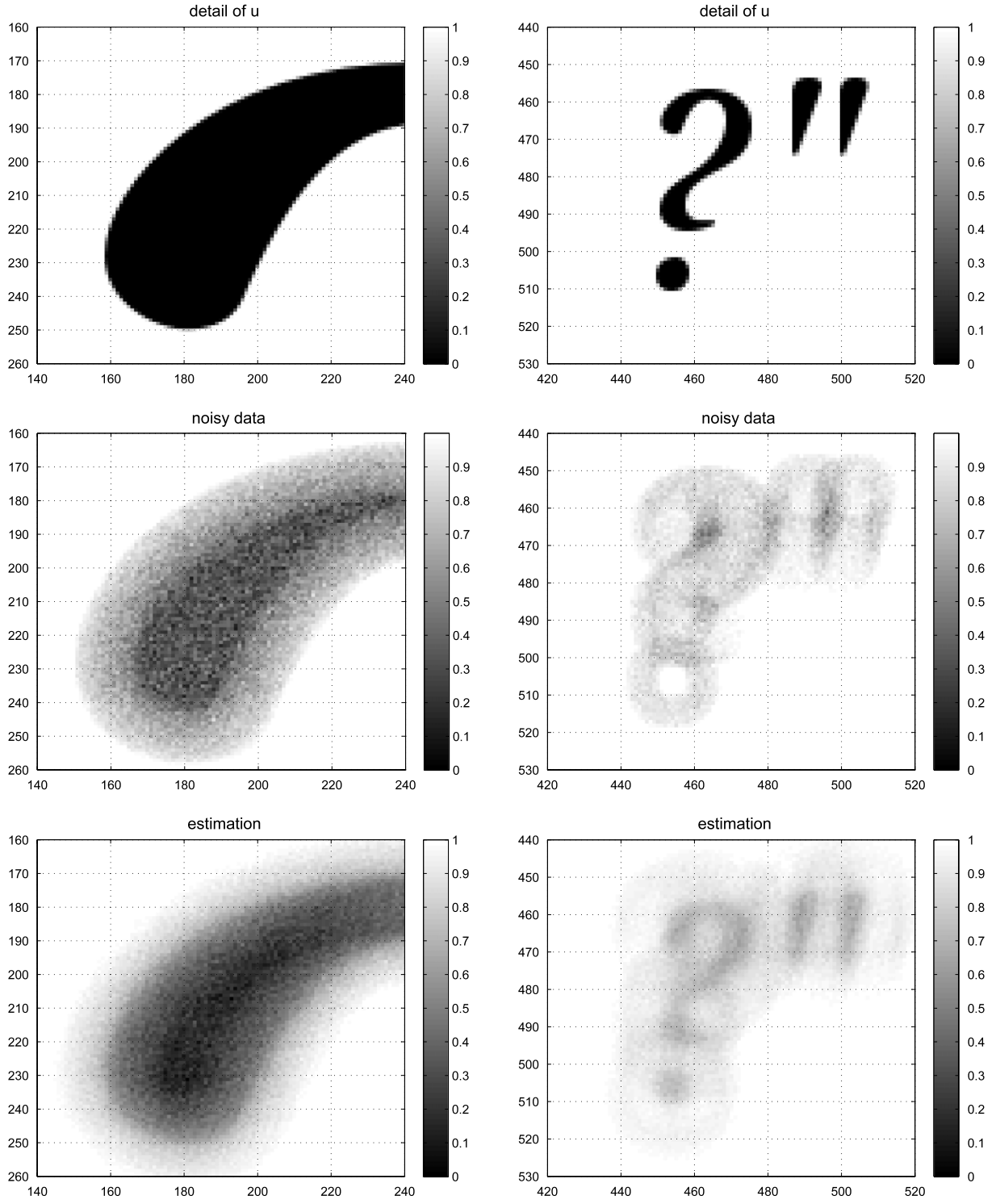

Fig. 5. Details to the second row in Fig. 4 ($T = \tau$). The left column shows the left top part of the big question mark and the right column shows the small question mark and the small apostrophe.

The value of τ is usually very small and hence the second case $\tau = T$ may not be reasonable. But this fact is not noticeable if the standard diffusion model is used, because the parameter τ does not appear there. In other words, whether the time T for the standard diffusion model with diffusion constant D is large or small cannot be derived from the value of D. Thus there

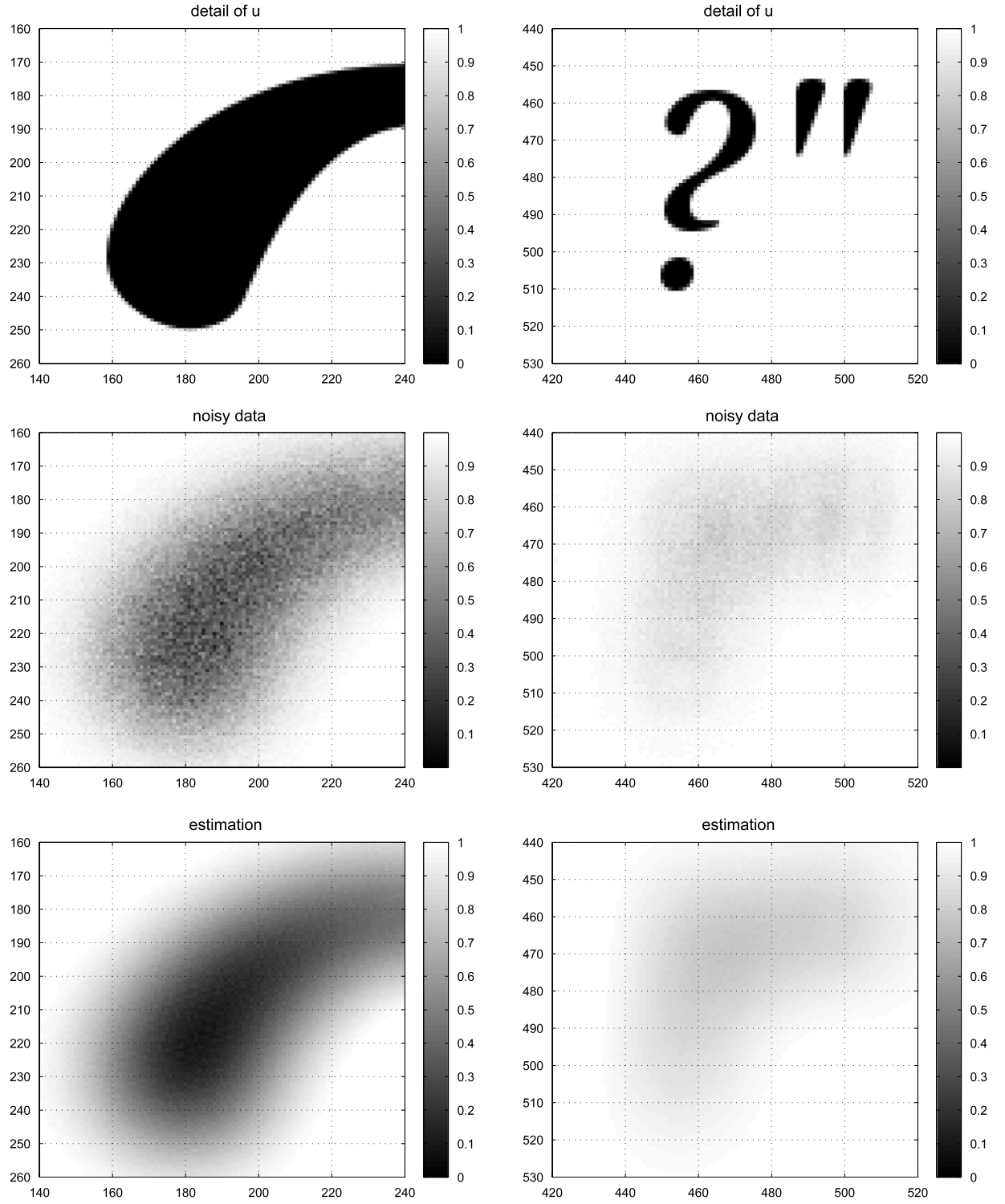

Fig. 6. Details to the third row in Fig. 4 ($T = 3\,\tau$). The left column shows the left top part of the big question mark and the right column shows the small question mark and the small apostrophe.

are cases where the standard backwards diffusion model can be numerically solved, however, they may not be relevant for applications.

In particular, we see that a better understanding and numerical solution of direct and inverse problems might be achieved if causal models are used.

Appendix

We use the following notation for the Fourier transformation:

$$\hat{f}(\mathbf{k}) := \mathcal{F}\{f\}(\mathbf{k}) := (2\pi)^{-N/2} \int_{\mathbb{R}^N} e^{\mathrm{i}\,\mathbf{k}\cdot\mathbf{x}} f(\mathbf{x})\,\mathrm{d}\mathbf{x}.$$

By $\check{g}(\mathbf{x})$ and $\mathcal{F}^{-1}\{g\}(\mathbf{x})$ we denote the inverse Fourier transform.

In order to derive an analytic representation of the Fourier transform of the Green function of causal diffusion, we need the following two lemmata.

Lemma 1. *For $N \in \mathbb{N}$ with $N > 1$ and $j \in \mathbb{N}$, let*

$$I(N,j) := \int_{-\pi/2}^{\pi/2} \sin^j(\varphi)\cos^{N-2}(\varphi)\,\mathrm{d}\varphi.$$

If j is odd, then $I(N,j) = 0$ and if j is even, then

$$\frac{I(N,j)}{I(N,0)} = \frac{1\cdot 3\cdot 5\cdots(j-1)}{N\cdot(N+2)\cdot(N+4)\cdots(N+j-2)}. \tag{17}$$

Proof. The claim follows from Integration by Parts and Induction. □

Lemma 2. *Let*

$$\Upsilon_N(t) := \sum_{j=0}^{\infty} (-1)^j \cdot a_{2j} \cdot t^{2j} \quad \text{for } t \in (0,\infty) \tag{18}$$

with $a_0 = 1$ and

$$a_{2j} = \frac{1}{(2j)!}\,\frac{1\cdot 3\cdot 5\cdots(2j-1)}{N\cdot(N+2)\cdot(N+4)\cdots(N+2j-2)} \quad (j \in \mathbb{N}).$$

The series (18) is absolutely convergent and

$$\int_{S_1(\mathbf{0})} \frac{\delta(\mathbf{x}+c\,s\,\mathbf{y})}{|S_1(\mathbf{0})|}\,\mathrm{d}\sigma(\mathbf{y}) = \frac{\mathcal{F}^{-1}\{\Upsilon_N(|\cdot|\,c\,s)\}(\mathbf{x})}{(2\pi)^{N/2}} \quad \text{for } \mathbf{x} \in \mathbb{R}^N,\ s \in (0,\tau].$$

Proof. That the series representation (18) converges absolutely follows at once from the Quotient Criterion.

Let $\mathbf{x},\ \mathbf{k} \in \mathbb{R}^N$. From

$$\mathcal{F}\{\delta(\mathbf{x}+a_1\,\mathbf{y})\}(\mathbf{k}) = (2\pi)^{-N/2}\,e^{-\mathrm{i}\,a_1\,(\mathbf{k}\cdot\mathbf{y})} \quad (a_1 > 0 \text{ constant})$$

and

$$\int_{S_1(\mathbf{0})} e^{a_2\,(\mathbf{k}\cdot\mathbf{y})}\mathrm{d}\sigma(\mathbf{y}) = \int_{S_1(\mathbf{0})} e^{a_2\,|\mathbf{k}|\,(\mathbf{e}_1\cdot\mathbf{y})}\mathrm{d}\sigma(\mathbf{y}) \quad (a_2 \in \mathbb{C} \text{ constant}),$$

it follows that

$$\hat{g}(\mathbf{k},s) := \mathcal{F}\left\{\int_{S_1(\mathbf{0})} \frac{\delta(\cdot + c\,s\,\mathbf{y})}{|S_1(\mathbf{0})|}\,\mathrm{d}\sigma(\mathbf{y})\right\}(\mathbf{k}) = \int_{S_1(\mathbf{0})} \frac{e^{-\mathrm{i}\,(\mathbf{e}_1\cdot\mathbf{y})\,|\mathbf{k}|\,c\,s}}{(2\pi)^{N/2}\,|S_1(\mathbf{0})|}\mathrm{d}\sigma(\mathbf{y})$$

for $s \in [0,\tau]$ and $\mathbf{k} \in \mathbb{R}^N$. Instead of $\mathbf{e}_1$ we can also use anyone in $\{\mathbf{e}_2, \mathbf{e}_3, \ldots, \mathbf{e}_N\}$. Expanding the exponential function yields

$$(2\pi)^{N/2}\,\hat{g}(\mathbf{k},s) = \sum_{j=0}^{\infty} (-1)^j\,\frac{(|\mathbf{k}|\,c\,s)^{2j}}{(2j)!}\,d_{2j} \tag{19}$$

with

$$d_j := \int_{S_1(\mathbf{0})} \frac{(\mathbf{e}_1\cdot\mathbf{y})^j}{|S_1(\mathbf{0})|}\,\mathrm{d}\sigma(\mathbf{y}) \quad \text{for } j \in \mathbb{N}.$$

We see at once that $d_j = 0$ if j is odd and $d_0 = 1$. For the convenience of the reader, we consider the cases $N = 1$ and $N > 1$ separately.

(a) For $N = 1$ we have $\int_{S_1(\mathbf{0})} \mathrm{d}\sigma(\mathbf{y}) \equiv \int_{\mathbb{R}} (\delta(y-1) + \delta(y+1))\,\mathrm{d}y$ and $|S_1(\mathbf{0})| = 2$, and thus

$$d_j = \frac{1^j + (-1)^j}{2} = \begin{cases} 1 & \text{if } j \text{ is even} \\ 0 & \text{if } j \text{ is odd.} \end{cases}$$

Inserting this into the series representation yields the claim.

(b) Let $N > 1$. The surface measure of the N-dimensional orthogonal coordinate system (cf. [31])

$$(r, \varphi_1, \ldots, \varphi_{N-1}) \in [0,\infty) \times (-\pi, \pi) \times (-\pi/2, \pi/2)^{N-2}$$

is given by $\mathrm{d}\sigma = r^{N-1}\,\mathrm{d}\varphi_1 \prod_{l=2}^{N-1} \cos^{l-1}(\varphi_l)\,\mathrm{d}\varphi_l$. From this we obtain $d_j = \frac{I(N,j)}{I(N,0)}$ with $I(N,j)$ defined as in Lemma 1. This and Lemma 1 implies $d_{2j-1} = 0$, $d_0 = 1$ and

$$d_{2j} = \frac{1 \cdot 3 \cdot 5 \cdots (2j-1)}{N \cdot (N+2) \cdot (N+4) \cdots (N+2j-2)} \quad \text{for } j > 0.$$

Inserting this into the series (19) yields the claimed series.

This concludes the proof. □

The following theorem enables us to specify the space Fourier transform of the Green function of causal diffusion for every dimension N and to prove some compactness results for the forward operator of causal diffusion.

Theorem 9. *Let $N \in \mathbb{N}$ with $N \geq 3$ and $t > 0$. The function Υ_N defined as in (18) satisfies*

$$\Upsilon_N(t) = -\frac{(N-2)}{t}\,\Upsilon'_{N-2}(t) \tag{20}$$

with

$$\Upsilon_1(t) = \cos(t) \quad \textit{and} \quad \Upsilon_2(t) = \mathrm{J}_0(t).$$

Here J_0 denotes the Bessel function *of first kind and order zero. Moreover, we have*

$$|\Upsilon_N(t)| \leq C_N\, t^{-(N-1)/2} \quad \textit{for sufficiently large } t \tag{21}$$

and some constant $C_N > 0$.

Proof. The relation between Υ_N and Υ'_{N-2} follows at once from the series representation (18). Moreover,

(a) if $N = 1$, then $a_{2j} = \frac{1}{(2j)!}$ and thus $\Upsilon(t) = \cos(t)$ and

(b) if $N = 2$, then $a_{2j} = \frac{1}{[2^j (j!)]^2}$ which implies $\Upsilon(t) = \mathrm{J}_0(t)$ (cf. [26]).

In order to prove the estimation we use

$$\frac{(t^{N-2}\,\Upsilon_N(t))'}{(N-2)\,t^{N-3}} = \Upsilon_{N-2}(t), \tag{22}$$

which follows from the series representation (18). We perform a proof by induction. Since $\cos(t)$ is bounded and the Bessel function $\mathrm{J}_0(t)$ satisfies the asymptotic behavior (cf. [32])

$$\mathrm{J}_0(t) \asymp \sqrt{\frac{2}{\pi\, t}}\, \cos\left(t - \frac{\pi}{4}\right) \quad \text{for } t \to \infty, \tag{23}$$

the estimation holds for $N = 1$ and $N = 2$. We assume that the estimation (21) holds and prove

$$|\Upsilon_{N+2}(t)| \leq C_{N+2}\, t^{-(N+1)/2} \quad \text{for sufficiently large } t.$$

From (20) and (22) we get

$$\begin{aligned} |\Upsilon_{N+2}(t)| &= \left|\frac{N}{t}\,\Upsilon'_N(t)\right| \leq \frac{N\,(N-2)}{t^2}\,(|\Upsilon_N(t)| + |\Upsilon_{N-2}(t)|) \\ &\leq \frac{N\,(N-2)\,(C_N + C_{N-2})}{t^{(N+1)/2}}, \end{aligned}$$

which proves the claim. □

References

[1] H.W. Engl, W. Rundell (Eds.), Inverse Problems in Diffusion Processes, SIAM, Philadelphia, 1995.
[2] A. Elayyan, V. Isakov, On an inverse diffusion problem, SIAM J. Appl. Math. 57 (1997) 1737–1748.
[3] O. Dorn, A transport-backtransport method for optical tomography, Inverse Problems 14 (1998) 1107–1130.
[4] V. Isakov, S. Kindermann, Identification of the coefficient in a one-dimensional parabolic equation, Inverse Problems 16 (2000) 665–680.
[5] V.A. Markel, J.C. Schotland, Inverse problem in optical diffusion tomography. I. Fourier–Laplace inversion formulas, J. Opt. Soc. Am. A Opt. Image Sci. Vis. 18 (6) (2001) 1336–1347.
[6] Y.A. Gryazin, M.V. Klibanov, T.R. Lucas, Imaging the diffusion coefficient in a parabolic inverse problem in optical tomography, Inverse Problems 15 (1999) 373–397.
[7] H. Ammari, E. Iakovleva, H. Kang, K. Kim, Direct algorithms for thermal imaging of small inclusions, Multiscale Model. Simul. 4 (4) (2005) 1116–1136.
[8] Y. Ahmadizadeh, Numerical solution of an inverse diffusion problem, Appl. Math. Sci. 1 (18) (2007) 863–868.
[9] B.M.C. Hetrick, R. Hughes, E. McNabb, Regularization of the backwards heat equation via heatlets, Electron. J. Differential Equations 2008 (130) (2008) 1–8.
[10] Hui Wei, Wen Chen, Hongguang Sun, Xicheng Li, A coupled method for inverse source problem of spatial fractional anomalous diffusion equations, Inverse Probl. Sci. Eng. 18 (7) (2010) 945–956.
[11] M. Addam, An inverse problem for one-dimensional diffusion transport equation in optical tomography, 2011, Preprint.
[12] H. Ammari, E. Bossy, V. Jugnon, H. Kang, Reconstruction of the optical absorption coefficient of a small absorber from the absorbed energy density, SIAM J. Appl. Math. 71 (3) (2011) 676–693.
[13] H. Ammari, E. Bretin, J. Garnier, A. Wahab, Time reversal in attenuating acoustic media, in: Mathematical and Statistical Methods for Imaging, in: Contemp. Math., vol. 548, Amer. Math. Soc., Providence, RI, 2011, pp. 151–163.
[14] H. Ammari, E. Bretin, J. Garnier, A. Wahab, Noise source localization in an attenuating medium, SIAM J. Appl. Math. 72 (1) (2012) 317–336.
[15] V. Isakov, Inverse Source Problems, in: Math. Surveys and Monographs Series, vol. 34, AMS, Providence, RI, 1990.
[16] H.W. Engl, M. Hanke, A. Neubauer, Regularization of Inverse Problems, Kluwer Academic Publishers, Dordrecht, 1996.
[17] A. Kirsch, An Introduction to the Mathematical Theory of Inverse Problems, Springer Verlag, New York, 1996.
[18] V. Isakov, Inverse Problems for Partial Differential Equations, Springer Verlag, New York, 1998.
[19] J. Weickert, Anistropic Diffusion in Image Processing, Teubner Stuttgart Verlag, Stuttgart, 1998.
[20] F. Natterer, F. Wübbeling, Mathematical Methods in Image Reconstruction, Society for Industrial and Applied Mathematics (SIAM), Philadelphia, PA, 2001.
[21] A.K. Louis, Inverse und Schlecht gestellte Probleme, Teubner Verlag, Stuttgart, 1994.
[22] F. Guichard, J.-M. Morel, R. Ryan, Contrast Invariant Image Analysis and PDE's, in: Lecture Notes, 2004, See http://mw.cmla.ens-cachan.fr/morel/.
[23] G. Sapiro, Geometric Partial Differential Equations and Image Analysis, Cambridge University Press, Cambridge, 2006.
[24] O. Scherzer, M. Grasmair, H. Grossauer, M. Haltmeier, F. Lenzen, Variational Methods in Imaging, Springer-Verlag, New York, 2009.
[25] R. Kowar, On the causality of real-valued semigroups and diffusion, Math. Methods Appl. Sci. 35 (2012) 207–227. arXiv:1102.3280v1 [math.AP].
[26] H. Heuser, Gewöhnliche Differentialgleichungen, Teubner, Stuttgart, 1989, (2. Auflage).
[27] L. Hörmander, The Analysis of Linear Partial Differential Operators I, second ed., Springer Verlag, New York, 2003.
[28] H.W. Alt, Lineare Funktionalanalysis, Springer Verlag, New York, 2000, (4. Auflage).
[29] M. Griebel, S. Knapek, G. Zumbusch, A. Caglar, Numerische Simulation in der Moleküldynamik, Springer-Verlag, New York, 2004.
[30] C. Gasquet, P. Witomski, Fourier Analysis and Applications, Springer Verlag, New York, 1999.
[31] U. Storch, H. Wiebe, Lehrbuch der Mathematik. Band III, Wissenschaftsverlag, Mannheim, 1993.
[32] I.N. Bronstein, K.A. Semendjajew, Taschenbuch der Mathematik, Harri Deutsch Verlag, Thun, Frankfurt, Main, 1979.